JOM, Vol. 72, No. 11, 2020
https://doi.org/10.1007/s11837-020-04331-0

Comparison of MnO_2 and ZnO Additives on Zircon Decomposition and Formation of Solid Solution

HUDSA MAJIDIAN,[1,2] LEILA NIKZAD,[1] and MOHAMMAD FARVIZI[1]

1.—Ceramic Department, Materials and Energy Research Center, Alborz, Iran. 2.—e-mail: h-majidian@merc.ac.ir

In this paper, the effects of MnO_2 and ZnO additives on zircon decomposition were investigated. The substitution of Mn and Zn into zircon lattices and the formation of solid solutions are discussed. The additives were added at 0–4 wt.% to zircon. The phase composition, physical properties, and microstructural changes for the sintered samples were characterized. Results of Rietveld refinement analysis showed that 1 wt.% of both additives retarded the decomposition of zircon. Further addition of additives slightly accelerated the zircon decomposition and improved sample densification. X-ray diffraction peaks of zircon were shifted to higher angles by the addition of MnO_2, whereas ZnO did not alter zircon peaks. Energy dispersive spectroscopy analysis detected the presence of Mn and Zn in zircon grains. ZnO has a lower solubility than MnO_2 in zircon, leading to the formation of a higher fraction of secondary phases, in turn leading to the suppression of grain growth.

INTRODUCTION

Zircon ($ZrSiO_4$) is an interesting ceramic material due to its high stability, good corrosion resistance, high melting point, good hardness, low thermal conductivity, and excellent thermal shock resistance. Zircon, as a common refractory material, is widely used for high-temperature applications and industries such as iron and steel production, energy technology, and protective coatings.[1–3]

The decomposition of zircon at elevated temperatures is one of the most challenging topics in the production of zircon refractories and composites. The decomposition temperature is important for the prediction of lifetimes of zircon and zirconia-based refractories.[4] The decomposition temperature of zircon depends on several factors, such as purity and fineness of the zircon.[1] This temperature is reported to be about 1673 ± 10°C, which is based on heat treatment experiments conducted on natural and synthetic zircon raw materials with known grain sizes and impurity levels, as well as zircon single crystals.[2]

(Received January 18, 2020; accepted August 17, 2020; published online September 2, 2020)

Zircon decomposition has been investigated to increase the working temperature of zircon refractories. Using zircon for high-temperature applications strongly depends on accurate knowledge about its thermal stability. There are some studies on the thermal stability of zircon without any additives.[4–6] However, research is limited regarding the influence of oxides on the decomposition of zircon. Anseau et al.[7] measured the degree of zircon decomposition and found that it starts between 1525°C and 1550°C and accelerates at 1650°C. Pavlik et al.[8] studied the decomposition of pure and impure zircon and reported that impure zircon decomposed after 8 h at 1285°C, while the decomposition of pure zircon particles was still incomplete. Sarkar and Baskey[5] evaluated the effect of using 1 wt.% of different additives (alumina, magnesia, titania, and iron oxide) on the densification and decomposition characteristics of zircon. The results of their study indicated that these additives had a negligible effect on the decomposition of zircon, but they improved densification behavior. The formation of the solid solution was not considered in their studies. In another study, the effects of adding 1 wt.% of MgO, Fe_2O_3, MnO, TiO_2, CaO, Al_2O_3, and Cr_2O_3 additives on the sintering temperature of zircon were investigated. The results showed that Fe_2O_3 had a beneficial effect on decreasing the

sintering temperature to 1500°C, but it had a coloring effect on zircon bodies, which limited its use. Adding 1 wt.% of MgO and TiO_2 could also decrease the sintering temperature down to 1500–1550°C. However, they did not investigate the decomposition of zircon in their study.[1]

The presence of oxide additives in zircon has a remarkable influence on its decomposition and sintering behavior. In many cases, sintering additives would segregate at grain boundaries and form a glassy phase.[9,10] MnO_2, as one of the typical additives, has been used in alumina, zircon, or zirconia ceramics as an accelerator of the sintering rate.[9–11] ZnO can also be used as an additive or a sintering aid for many ceramics,[12–15] and its effect on the improvement of densification, chemical stability, and electrical properties of ceramics has been reported. Zhou et al.[11] reported that MnO_2 forms a solid solution in zirconia crystal, and may increase the lattice defects of zirconia, leading to the reduction of diffusion activation energy. Therefore, the substitution of Mn in Zr sites results in fast diffusion paths during the sintering process. It was also reported that ZnO was effective in better densification of ZrO_2 samples through a viscous flow sintering.[16]

Zr can be substituted by some elements such as Hf, Pu, U, Th, etc.; however, there is little knowledge about miscibility in most of these systems.[17] Studies have mostly focused on the solid solution of Hf^{4+}, U^{4+}, and Th^{4+} in zircon.[18] Considering the remarkable advantages of increasing the decomposition temperature of zircon ceramics and refractories, the present study aimed to investigate the influence of adding small amounts of metal oxides (manganese and zinc oxides) on the decomposition temperature and densification of zircon. In this case, the additive quantities should be correctly chosen to avoid the undesired effect of liquid phase formation. The liquid phase has been reported to disappear during heat treatment if the appropriate amounts of additives are used.[19] In fact, the decomposition temperature was evaluated in this study using various amounts of two useful additives at different sintering temperatures. Also, it is known that solid solution formation can affect the physical properties of ceramics.[20] Therefore, the formation of the solid solution of Mn and Zn in zircon and its effect on the final composition, density, microstructure, and grain growth were investigated and compared.

MATERIALS AND METHODS

Materials

Zircon powder (Global, 5 μm, 99.8% purity), zinc oxide (Germany, $<$ 20 μm, 99% purity), and MnO_2 (South Africa, $<$ 20 μm, 99% purity) were used as raw materials. Dolapix CE-64 was also used as the process control agent for the milling media.

Sample Preparation and Sintering

First, zircon powder was milled for 24 h in a planetary mill (200 rpm, ball to powder ratio of 10:1) to reduce the particle size and improve its sinterability. The samples were prepared by mixing the milled zircon by 0, 1, 2, and 4 wt.% of additive powder with 0.5 wt.% of the dissolved Dolapix in water using a planetary mill (250 rpm) for 2 h. After ball milling, the mixtures were dried on a magnetic heater, then were granulated by passing through 60- and 100-mesh sieves. Zircon granules were pressed uniaxially at 250 MPa. Green samples were heated at 1450°C, 1550°C, and 1650°C with a holding time of 3 h. Sintered samples were coded according to the amount of additive and sintering temperature (see supplementary Table SI).

Characterization

Density and apparent porosity of the sintered samples were determined using the standard water adsorption method (ASTM C20). At least 5 samples were tested to obtain a mean value for each test. Crystalline phases in heated samples were characterized by X-ray diffraction (XRD, Siemens, D500 system) using Cu Kα radiation, working with 30 kV accelerating voltage. Moreover, a quantitative analysis of prepared samples was performed using the Rietveld refinement technique with Material Analysis Using Diffraction (MAUD) software which works using the least-squares method. Instrumental broadening was removed using a defect-free silicon sample. In all refinements, "Sig." and "R" values were less than 2 and 10, respectively. The degree of zircon decomposition was based on measuring the ratio of the decomposed zirconia to the unreacted zircon.[8] The microstructure of the sintered samples was observed by scanning electron microscopy (SEM, VEGA II SCAN) on the polished and thermally etched (150°C below the sintering temperature, 20 min) surfaces.

RESULTS AND DISCUSSION

Xrd

XRD Patterns

XRD patterns of zircon sintered without any additives (Z0 samples) and with different amounts of additives (ZZ and ZM samples) are shown in Supplementary Fig. S1. Tetragonal (Zt) and monoclinic (Zm) zirconia peaks were observed as well as the zircon peaks. It can be seen that in all samples the zircon dissociation was increased at 1650°C. According to thermodynamic calculations, zircon decomposes into ZrO_2 and SiO_2 oxides at about 1676 ± 7°C[3]: there is no general agreement on this temperature. After zircon decomposition, zirconia appears in the tetragonal form at the sintering temperature and is usually transformed to the monoclinic structure by cooling down to room

temperature. Most experiments revealed that the decomposition of zircon leads to the formation of monoclinic zirconia and glassy phase as the final products.[2,8] Figure 1S shows that part of the tetragonal zirconia remains at room temperature, indicating that zirconia has been partially stabilized in all samples. The stabilization of Zt is due to the presence of additives and fine particle sizes of raw material.[21] Comparing the XRD patterns of Z0 samples and those containing additives shows that MnO_2 and ZnO had a remarkable influence on the XRD pattern of zircon. Awaad et al.[1] reported that adding 1 wt.% of metal oxides (such as MnO) did not cause any variation in the XRD pattern of zircon; also, they did not observe a tetragonal zirconia peak or silica, while the results of the present study showed that only 1 wt.% of MnO_2 and ZnO additives are capable of retarding the decomposition of zircon even at a high temperature (1650°C). Formation of Zn_2SiO_4 (31.5° and 34°) and Mn_2SiO_4 (31° and 35°) may be considered; however, their XRD peaks overlap completely with zircon, and the formation of these phases cannot be proved with this characterization method.

Phase Composition of ZZ Samples

Figure 1 shows the Rietveld analysis of XRD patterns for zircon sintered with ZnO. The Rietveld refinement method using MAUD software was conducted on the XRD patterns of all composites to more precisely investigate the quantities of phases of the prepared composites. Figure 1a shows that increasing the sintering temperature leads to a greater decomposition of zircon (less zircon remaining) which is accompanied by the formation of Zm (Fig. 1b) or Zt (Fig. 1c). Kaiser et al.[2] showed the strong dependence of zircon decomposition on temperature. Due to the incorporation of the additives, a lower degree of zircon decomposition was observed for all the samples. The amount of remaining zircon increased from 42% to 83% (ZZ1-1650) and from 92% to 96.7% (ZZ1-1450) after the addition of 1 wt.% ZnO. This shows the strong influence of ZnO additive on the thermal stability of zircon. The amounts of Zt (9.0% to 4 wt.%) and Zm (49% to 13 wt.%) were also found to be decreased in the ZZ1-1650 sample. Increasing the amount of ZnO up to 2 wt.% led to a slight increase in remaining zircon and Zt. The highest amount of Zt (4.5 wt.%) was obtained in the ZZ2-1650 sample. Further increase in the amount of ZnO (up to 4 wt.%) resulted in a little increase of zircon stability but the Zt remained stable. The formation of Zt due to the addition of ZnO to zirconia has also been observed by other researchers.[22,23] Therefore, it can be concluded that the addition of ZnO prohibits zircon decomposition, probably due to the formation of a solid solution that lowers the likelihood of zircon lattice transformation, or reaction of ZnO with impurities such as Al, and formation of a secondary phase. The formation of a secondary phase such as $ZnAl_2O_4$ has been reported elsewhere.[24]

Phase Composition of ZM Samples

Figure 2 shows the Rietveld analysis of XRD patterns for zircon sintered with MnO_2. The same trend as for ZnO is also observed with the addition of MnO_2. The amount of remaining zircon increased from 42% (Z0-1650) to 92% (ZM1-1650). The remaining zircon was more than 90% in other ZM samples. Adding 1 and 2 wt.% of MnO_2 additive resulted in the lowest amounts of Zm and Zt (Fig. 2b and c), meaning that the suppression of the decomposition of zircon has occurred. However, it is revealed that increasing the additive content up to 4 wt.% results in the stabilization of Zt. The formation of Zm was observed to be decreased by more addition of MnO_2. Tetragonal zirconia stability of 1 wt.% MnO_2-doped TZP was also reported to be sensitive to the sintering temperature, and it decreased at 1400°C.[10] Studies have reported that adding MnO_2 to zirconia is beneficial for the stability of Zt.[11,25] The reason for this is that MnO_2 (or ZnO) dissolves into the ZrO_2 and creates oxygen vacancies.[26–28] Oxygen vacancies are responsible for the stabilization of tetragonal zirconia.[29]

Formation of Solid Solution

The study of the elemental substitution in zircon revealed that cations can be substituted at the Zr or Si sites.[30] Therefore, some degree of solid solution can be expected between zircon and the additives. As shown in Fig. 3a, at 1650°C, the position of the zircon peak was not changed by ZnO addition. This can be attributed to the similar ionic radius of Zn^{2+} (74 pm) and Zr^{4+} (72 pm). Some researchers have reported a minor change in the lattice parameters of stabilized zirconia by ZnO doping, due to this fact.[31–33] Investigations on the effect of ZnO addition on stabilized zirconia showed that ZnO dissolves in the ZrO_2 lattice.[26,27,34] Therefore, it may be concluded that Zn^{2+} can dissolve in the zircon lattice too, and a solid solution may be formed, but more precise studies are needed in this regard. According to the Hume-Rothery rules,[35] the solid solution occurs if the relative difference between the atomic radii of the two species is lower than 15%. The mismatch parameter between Zr (72 pm) and Zn (74 pm) radii is 2.8%. Also, a metal with a lower valency (Zn^{2+}) is more likely to dissolve in another metal with a higher valency (Zr^{4+}). Therefore, some degree of solid solution can be expected between zircon and ZnO; however, the different crystal structure of zircon (tetragonal) and ZnO (hexagonal) may the reason for a low solubility limit.

As shown in Fig. 3b, the zircon peak was shifted towards higher angles by MnO_2 addition (ZM4-1650 sample). This is attributed to the formation of a solid solution of MnO_2 in the zircon lattice. The mentioned solid solution has a different crystal

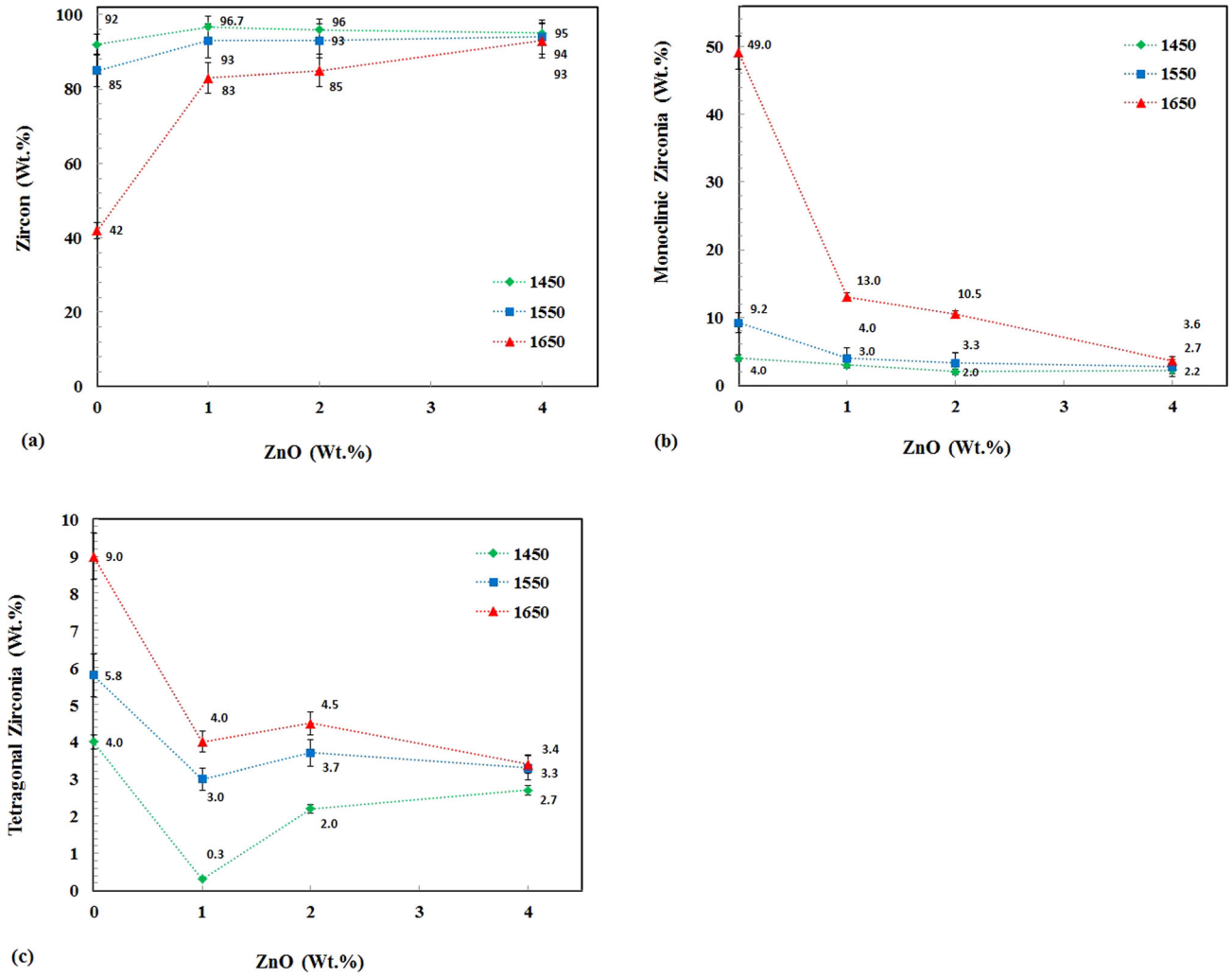

Fig. 1. (a) Zircon decomposition degree, (b) formation of monoclinic zirconia, (c) formation of tetragonal zirconia with ZnO additive.

lattice. If ions of lower radius substitute in a lattice (ionic radius of Mn^{4+} is 53 pm [29,36]), they will bring about a stretching stress leading to the shift of the XRD peaks to higher angles.[11,22] Accordingly, it can be concluded that a solid solution of Mn is formed in zircon. There are other studies on the shift of the zirconia peaks towards higher angles by the addition of MnO_2 which was also attributed to the formation of solid solution.[36–38] The MnO_2-ZrO_2 solid solution has been widely investigated; however, the present authors did not find any papers on the solid solutions of Mn^{4+} or Zn^{2+} in zircon.

Temperature is the most important factor in the formation of a solid solution. The formation of a solid solution is faster at a higher temperature.[20] Figure 3c and d show the effect of temperature on the XRD peak of ZZ1 and ZM1 samples, respectively. There is a little shift of the zircon peaks to lower angles by increasing the temperature. The zircon peak of the ZZ1-1650 sample is located at lower angles with respect to the ZZ1-1550 sample. The effect of temperature is also evident in Fig. 3d. The zircon peak of the ZM1-1650 sample is at a higher angle with respect to the ZM1-1550 and ZM1-1450 samples. This means that sintering temperatures higher than 1450°C are needed for the observation of zircon solid solution.

Microstructure

The SEM images related to the microstructure of the zircon samples are shown in Figs. S2 and S3. These images indicate the presence of zircon grains as well as dark areas or glassy phase. A porous microstructure was observed.

SEM of ZZ samples

Figure 4a and b show the microstructure of ZZ1-1550 and ZZ4-1550 samples at higher magnification. The small white grains are zirconia, and the light gray grains are the zircon matrix (Fig. 4c, d). Dark areas are the glassy phase (point *A*). Energy dispersive spectroscopy (EDS) of point *A* shows the high amount of Si and O present, along with lower

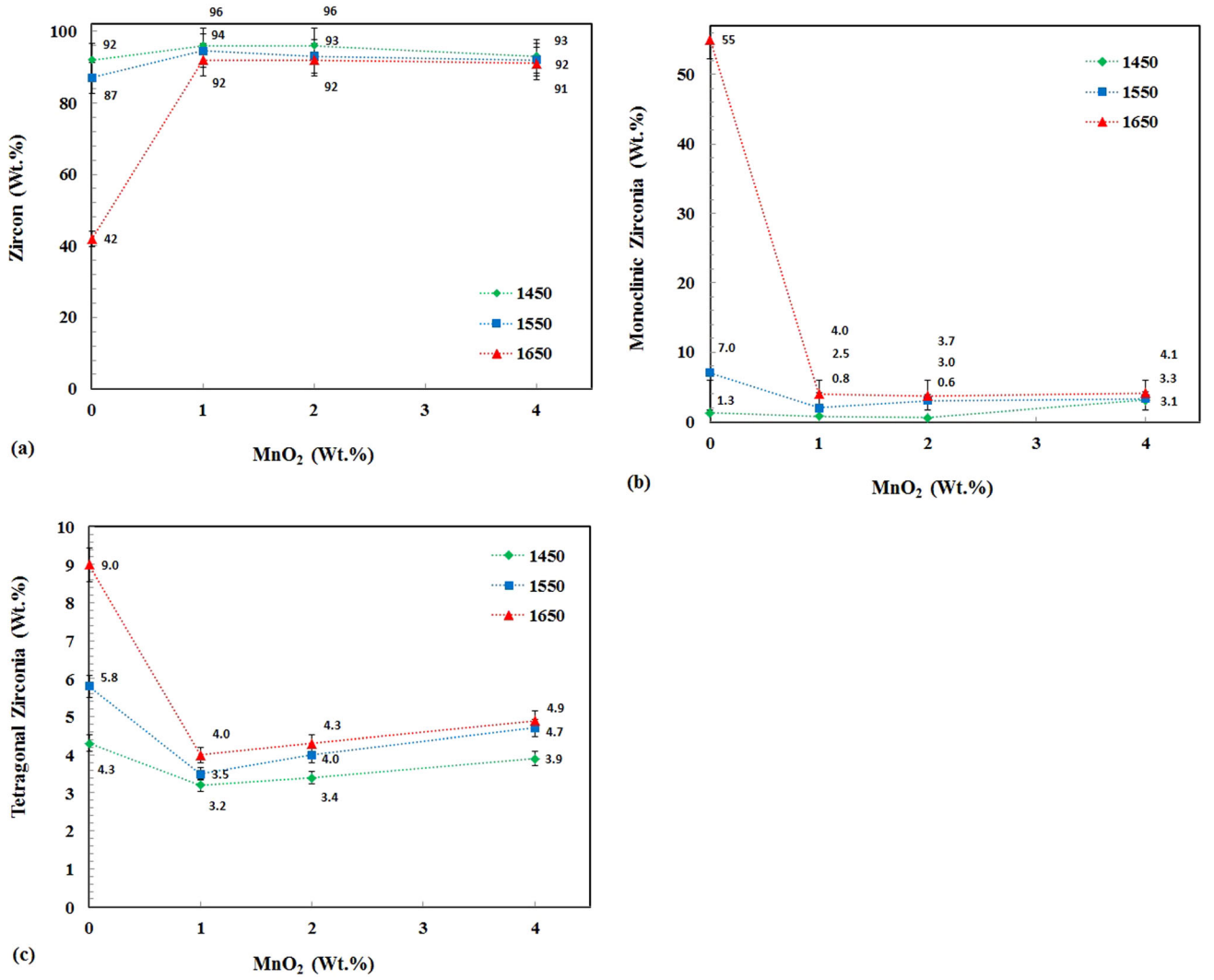

Fig. 2. (a) Zircon decomposition degree, (b) formation of monoclinic zirconia, (c) formation of tetragonal zirconia with MnO_2 additive.

amounts of Zr and Zn elements (Fig. 4e). A second phase was also observed in ZZ samples inside the glassy phase (arrows in Fig. 4a). This phase was more clearly observable in the ZZ4-1550 sample (Fig. 4b). EDS analysis of this phase indicates the presence of Zn, O, Si, and Al elements (Fig. 4f). Possibly, this is due to ZnO dissolution in zircon by forming Zn-rich grain boundaries, which increases the ion mobility of Zr^{4+} within and across the grain boundary region. Therefore, grain boundary diffusivity was activated and resulted in facilitating the consolidation of particles.[39] Other researchers indicated that the observed second phase is $ZnAl_2O_4$ or Zn_2SiO_4 spinel.[40,41]

SEM of ZM Samples

Figure 5a and b show the microstructure of ZM1-1550 and ZM4-1550 samples, respectively. Zircon and zirconia grains are indicated by gray and white grains, respectively. The EDS of the dark glassy phase (point *A*) is also shown in Fig. 5c. The second phase was clearly observed in the ZM-1550 sample (point *B* or arrows of Fig. 5b). EDS analysis of this phase indicates the combination of Mn, O, Si, and Al elements (Fig. 5d). The second phase, which has also been observed in SEMs by other researchers, indicates the formation of spinel ($MnAl_2O_4$).[42,43]

The ionic radii of Zn^{2+} and Mn^{4+} are equal to 74 and 53 pm, respectively.[44] Therefore, it can be concluded that the penetration of Mn^{4+} ions into the Zircon lattice (Zr^{4+} ionic radius is equal to 72 pm[44]) is easier than that of Zn^{2+}. Also, the atomic volume (the ratio of weight to density) of Mn is calculated to be about 7.6 cm^3/mol, which is less than that of Zn (9.2 cm^3/mol). The smaller atomic volume of Mn led to the higher diffusion rate of this element into the zircon lattice; therefore, it can be said that the penetration of manganese into the zircon lattice is more favorable than the zinc. Maybe this is why the secondary phase mentioned previously was clearly observed in all ZZ samples, but not in ZM1 samples. In the formation of solid solution,

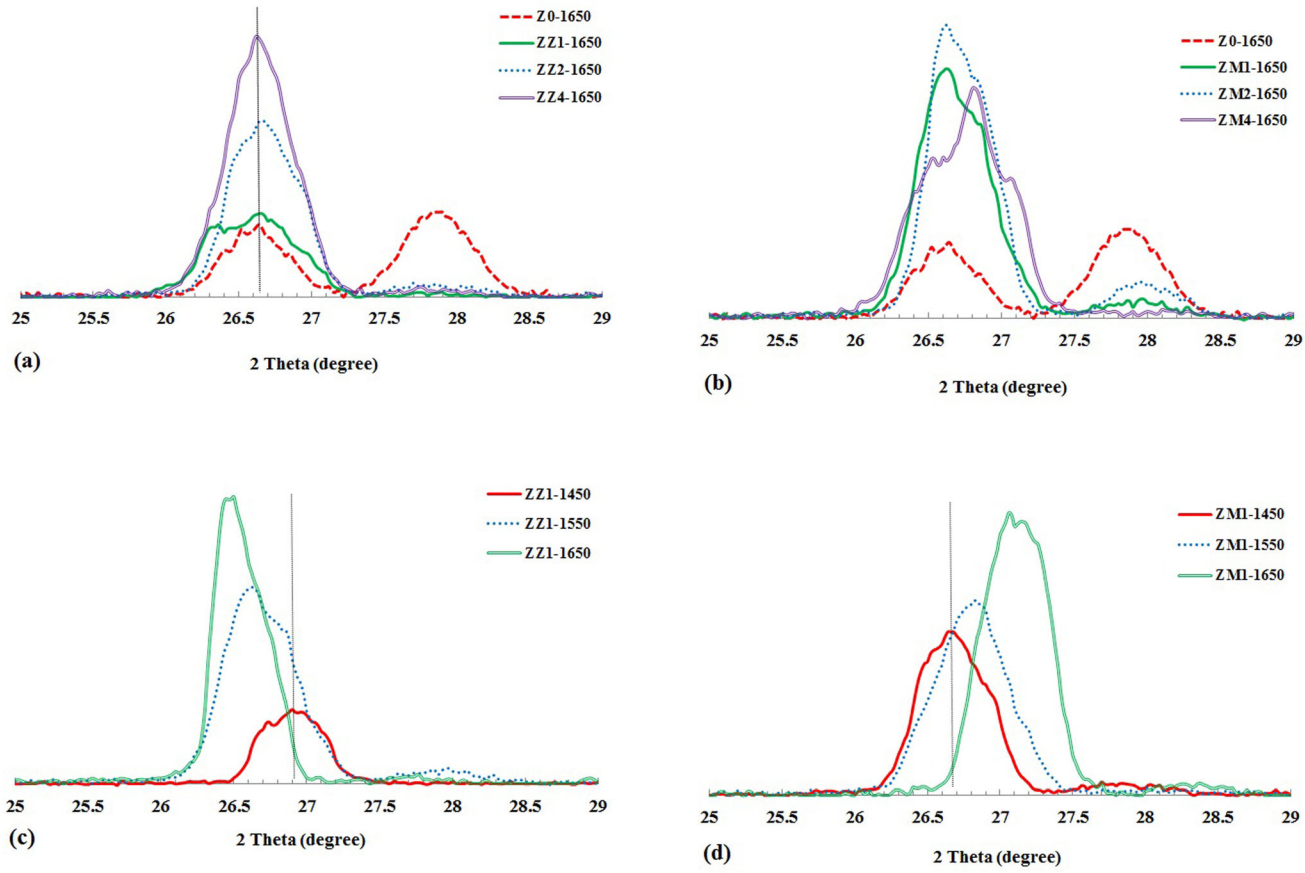

Fig. 3. Shifting of zircon peaks (a) ZZ-1650, (b) ZM-1650, (c) ZZ1, (d) ZM1 samples.

1 wt.% of MnO_2 was incorporated. However, the majority of ZnO doped into zircon resides at the grain boundaries as a secondary phase, because of the higher ionic radius of Zn^{2+} than Zr^{4+}, implying its low solubility in zircon lattice. The lower radius of Mn rather than Zr, the similarity between MnO_2 and zircon crystal structures (tetragonal), and the same valency of these elements (4+) can be considered to be favorable reasons for the formation of solid solutions of Mn in Zircon. On the other hand, Zn has a different crystal structure and valency; therefore, the formation of a solid solution of Zn in zircon would be expected to be less than that of Mn.

MAP Analysis of ZZ and ZM Samples

Grain boundary phases (dark gray areas shown by letter "*A*" in Figs. 4b and 5a) for each sample were analyzed by EDS (see supplementary Table SII and SIII). The amount of Mn increased in the glassy phase of the sintered samples by increasing the manganese oxide additive content, as well as the temperature. Seemingly, Mn had penetrated into the zircon lattice up to its solubility limit; beyond the solubility limit of Mn in zircon, extra Mn remained in the grain boundary. A similar trend was observed for the ZnO additive. Increasing the amount of zinc oxide additive resulted in an increase in the amount of Zn in grain boundary composition.

Figure 6 shows the map analysis of ZZ and ZM samples. Distribution of Zr, Si, O, Al, Zn, and Mn elements is reported here. As can be seen, Zr, Si, and O are distributed all over the grains, showing the presence of the zircon matrix. Brighter zirconia grains show a greater concentration of Zr element. Al is an impurity and appeared more in zircon grain boundaries. Indeed, the successful doping of Zn and Mn into the zircon lattice structure can be seen in these maps. Map analysis in Fig. 6a and b show that Zn is highly dispersed in zircon and it also exists in grain boundaries. This indicates the low solubility limit of Zn in zircon. According to the ZM4-1550 image (Fig. 6c), Mn is also distributted uniformly in the sample. The ZM4-1650 image (Fig. 6d) shows that Mn element (which is beyond the solubility limit) is more concentrated at the grain boundaries as well as the grains. This means that the solubility limit of Mn in zircon is less than 4 wt.%.

Grain Size

The interconnection of zircon grains is visible in the ZZ1-1550 and ZZ4-1550 samples, whereas zircon grains in the ZZ2-1550 sample appear more separated (Fig. S2). Separated or isolated zircon

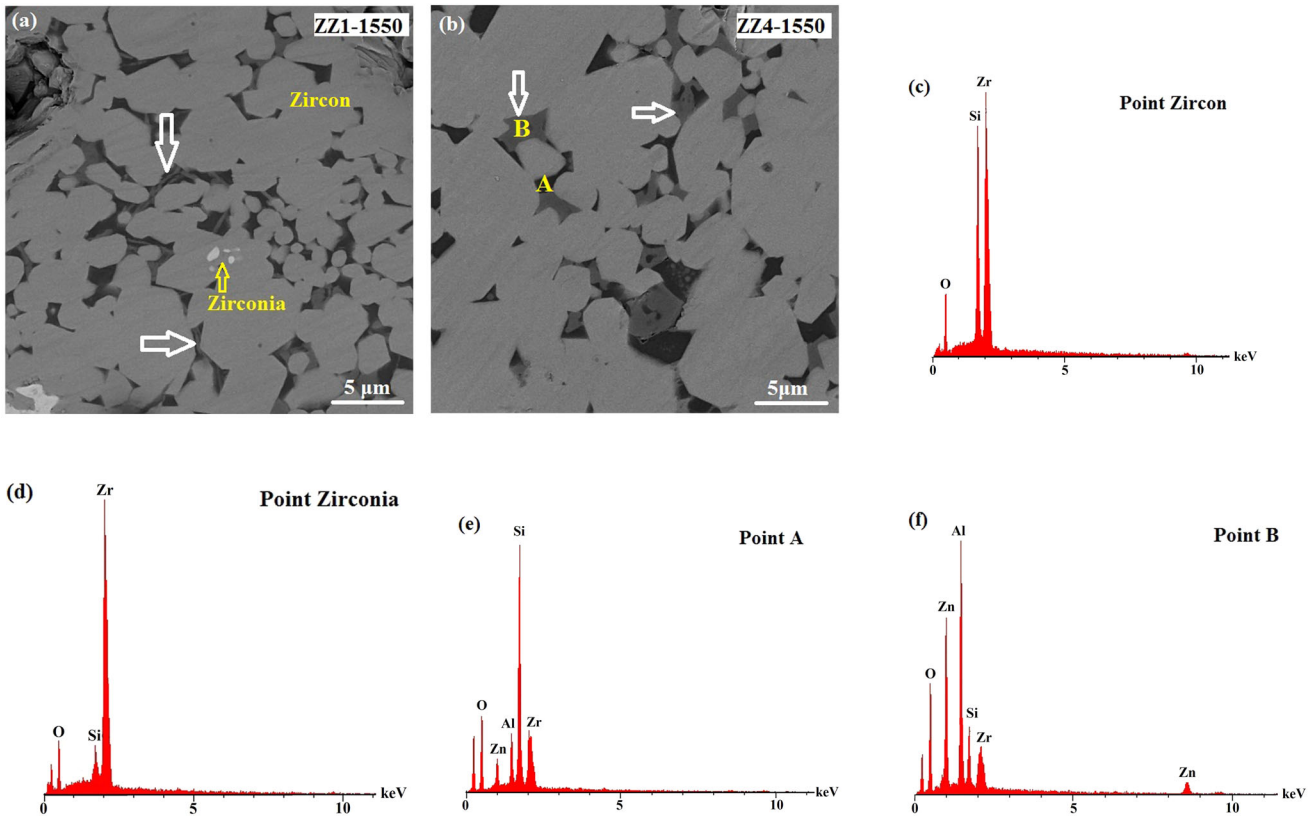

Fig. 4. Microstructure of (a) ZZ1-1550, (b) ZZ4-1550, and EDS analysis of (c) point zircon, (d) point zirconia, (e) point *A*, (f) point *B*.

grains means a higher degree of zircon decomposition. The higher temperature is responsible for more decomposition and hence the smaller size of the zircon grains. However, grain sizes of zircon were estimated by ImageJ software and it was found that zircon grain sizes of ZZ-1550 samples (7 μm) and ZZ-1650 samples (8 μm) were nearly the same. The zircon grain size of the Z0 sample was more than 20 μm, and this shows that ZnO addition can inhibit zircon grain growth. This is more obvious in the ZZ4-1550 sample. The SEM observation of Liu et al.[16] shows that the addition of ZnO has a strong effect on the microstructure and enhanced grain growth of zirconia. On the other hand, the beneficial effect of ZnO addition on the improvement of ZrO_2 morphology[31] and reduction of the grain size in YSZ[32] have been reported.

There were no remarkable differences between ZM samples (Fig. S3). The zircon grain sizes of ZM-1550 and ZM-1650 samples were about 12 μm and 10 μm, respectively. Extra grain growth of alumina and zirconia due to using manganese oxide as a sintering additive has been reported in previous studies[9,45,46]; however, fortunately, the grain growth was not observed in ZM samples. The influence of additives in decreasing the zircon grain size was more observable in the ZM4-1650 sample (5 μm).

The previous results demonstrate that the presence of ZnO leads to the formation of a new phase at the grain boundary of all ZZ-1550 and ZZ-1650 samples. It was also observed that the grain boundaries of only ZM-1650 samples include a segregated phase. This is why ZnO was more effective in the reduction of zircon grain size. These second phases can hinder the grain growth of zircon. Any grain boundary migration should be incorporated by Zn (or Mn) ions, indicating that it was harder for the grain boundary to move, which resulted in prohibition of grain growth. Mn_3O_4 was detected as the secondary phase in zirconia when the amount of manganese oxide was higher than the solubility limit.[36]

Porosity

The variation of apparent porosity for the zircon sintered with different amounts of additives is shown in Table I. Generally, the maximum density and sinterability is accompanied by lower porosity. Table I shows that the lower porosity is achieved at higher firing temperatures. The total density of zircon products is less than that of the reactant; therefore, the decomposition of zircon increases the porosity. Hence, additives can be beneficial in porosity reduction.

Porosity of ZZ Samples

The porosity of zircon samples sintered with ZnO additive (1 wt.%, 2 wt.%, or 4 wt.%) at 1450°C was

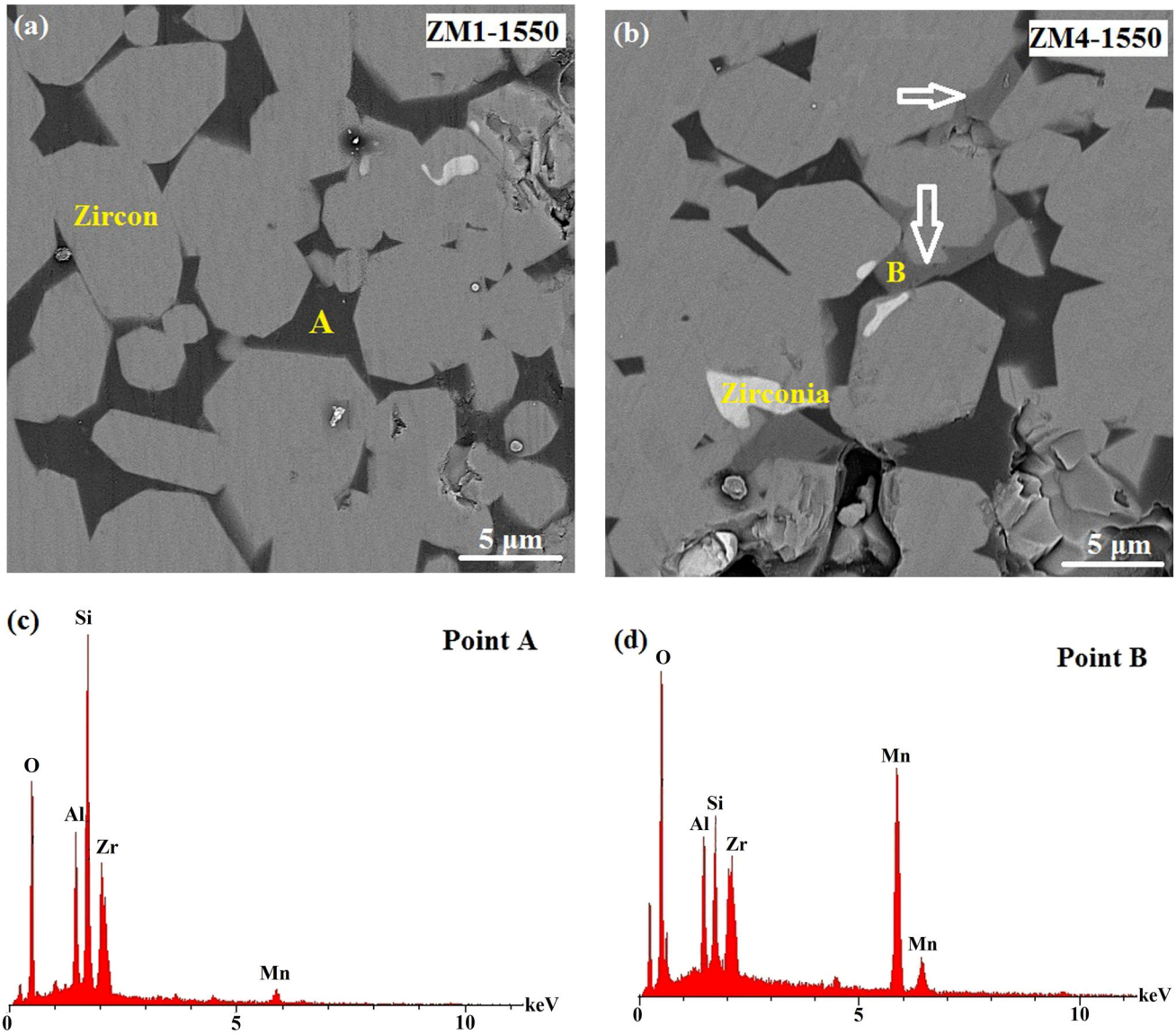

Fig. 5. Microstructure of (a) ZM1-1550, (b) ZM4-1550, and EDS analysis of (c) point *A*, (d) point *B*.

about 30% and did not change significantly by ZnO content. This means that the sintering temperature was too low for the densification of zircon and it cannot even be improved by ZnO addition. The porosity of the ZZ1-1550 sample was 24.9%; however, ZZ2-1550 showed a remarkable decrease in the porosity (17.2%) which indicates the positive effect of ZnO sintering aid at higher temperatures. The increase of the porosity of the ZZ4-1550 sample (24%) somehow related to the decomposition of zircon. The lower porosity of the ZZ1-1650 sample (17.9%) was due to an increase in the sintering temperature and higher consolidation. More zircon decomposition was observed for the ZZ2-1650 sample which was responsible for the higher porosity. It should be noted that the lower decomposition of zircon in the ZZ4-1650 sample resulted in lower porosity (21.9%) than in the ZZ2-1650 sample.

It has been reported that a small addition of ZnO was effective in reducing the sintering temperature and increasing the densification of ZrO_2 samples[23,27,31] through viscous flow sintering.[16] Probably, the viscous flow promotes the diffusivity rate of the zircon, thus ZnO can enhance the densification (ZZ2-1550). In addition, at lower ZnO content, the formation of the solid solution and inhibition of zircon decomposition are beneficial effects of ZnO. Despite these beneficial effects, there is a contradictory result in some samples, showing that adding ZnO inhibited the sintering process of zircon. The higher melting point of ZnO,[23] the formation of secondary phases at grain boundaries, and high sintering temperature which accelerates zircon decomposition are the reasons for lower densification. On the other hand, the ionic radius of Zn^{2+} is higher than Zr^{4+}. At high ZnO content, possibly Zn

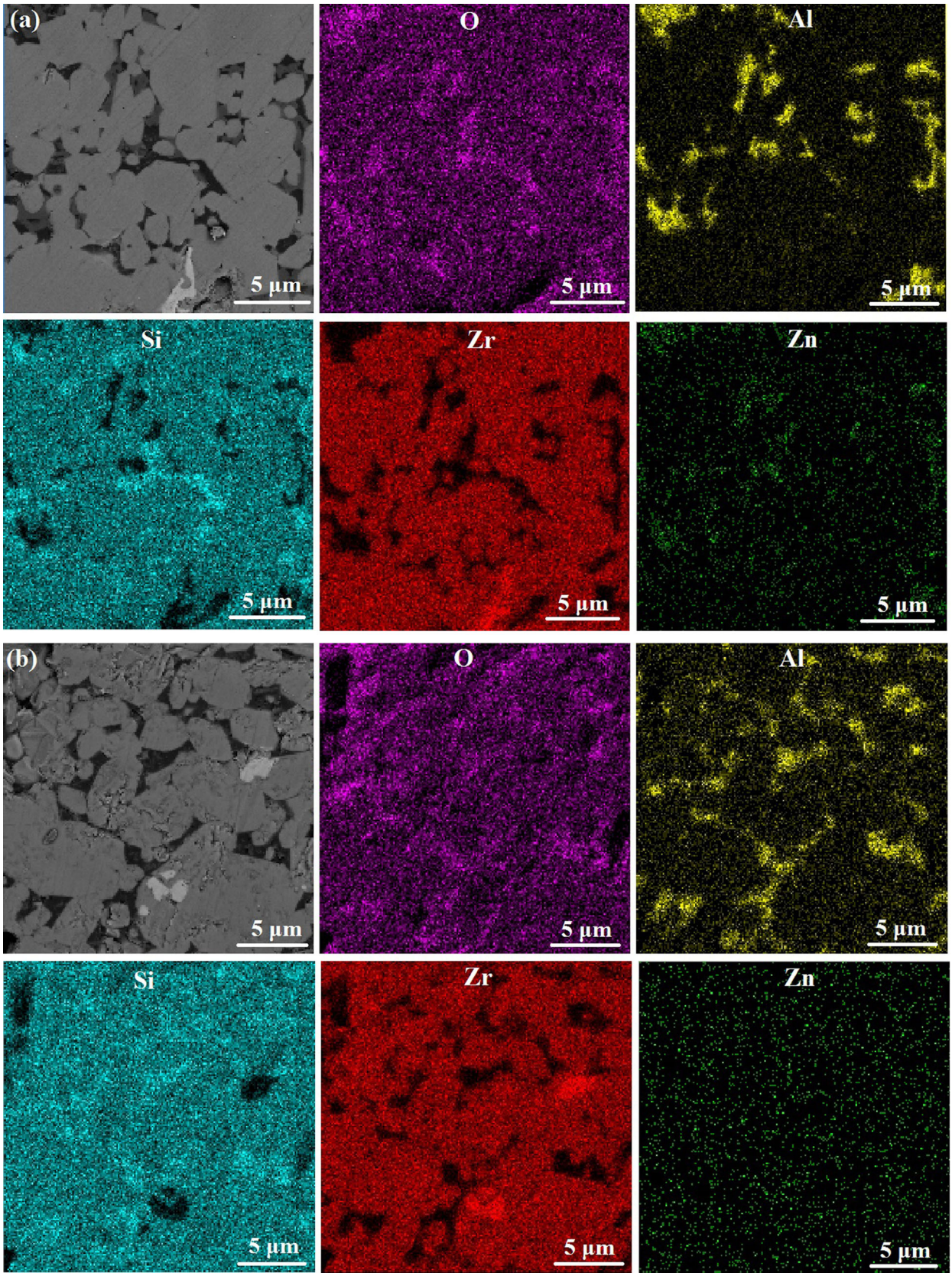

Fig. 6. Map analysis of (a) ZZ4-1550, (b) ZZ4-1650, (c) ZM4-1550, (d) ZM4-1650.

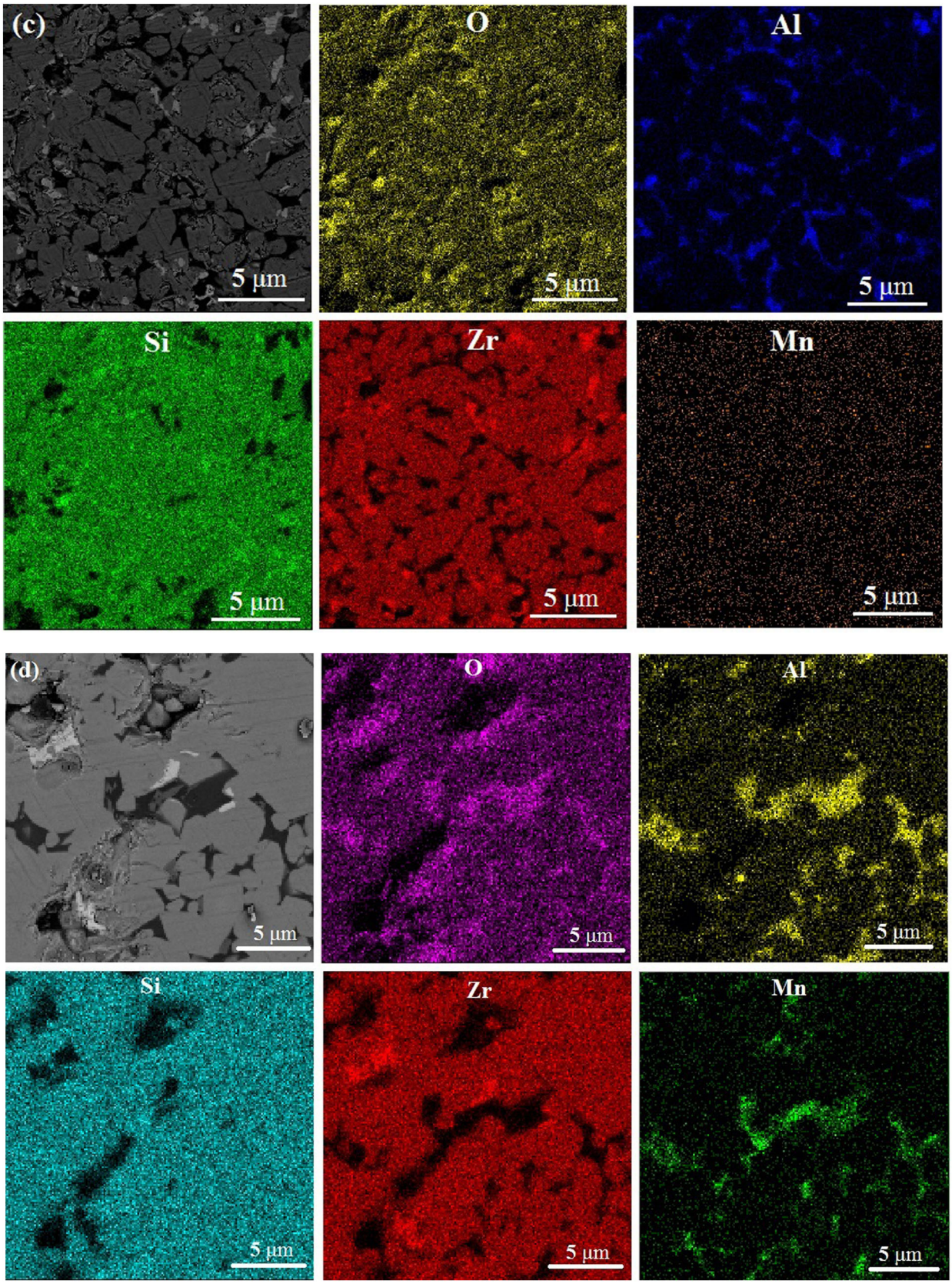

Fig. 6. continued

Table I. Porosity of the sintered zircon with additives (± 3%)

Sample code	1450°C	1550°C	1650°C
Z0	25.8	3.3	5.5
ZZ1	30.1	24.9	17. 9
ZZ2	29.3	17.2	24.7
ZZ4	32.3	24.0	21.9
ZM1	34.4	29.4	27.7
ZM2	30.5	30.8	19.3
ZM4	29.7	17.1	8.3

ions or the secondary phase sited in the grain boundaries, inhibit the migration of Zr and also suppress grain growth; therefore, the lower densification of zircon can be attributed to the high amount of ZnO at high temperature.

Porosity of ZM Samples

Table I shows that MnO_2 addition results in a decrease in zircon porosity. Previous studies reported the beneficial effect of MnO_2 in the densification of other ceramics such as zirconia.[10] Ramesh et al.[39] showed that MnO_2 doping resulted in relatively high density and enhanced the consolidation process of stabilized zirconia. A transient liquid phase was found in the MnO_2-doped zirconia during sintering in their work. Zhou et al.[11] reported that MnO_2 forms a solid solution in zirconia crystal, and may increase the lattice defects of zirconia, leading to a reduction of diffusion activation energy. Therefore, the substitution of Mn in Zr sites results in fast diffusion paths during the sintering process.[47] Formation of the solid solution and liquid phase[5] as well as inhibition of zircon decomposition can be considered to be the reasons for the improvement of zircon densification.

CONCLUSION

The present study aimed to evaluate zircon decomposition and formation of solid solution using 1 wt.%, 2 wt.%, and 4 wt.% of ZnO and MnO_2 as additives at different temperatures. Using 1 wt.% of these additives retarded zircon decomposition and developed its thermal stability. Maximum decomposition was achieved at a temperature of 1650°C. Formation of tetragonal zirconia was promoted as the ZnO or MnO_2 amount increased up to 2 wt.% or 4 wt.%, respectively. The sintered zircon using 4 wt.% of MnO_2 or 2 wt.% of ZnO had the lowest porosity. There was a little shift of the XRD peaks of zircon toward higher angles through the use of MnO_2; however, ZnO did not result in any remarkable shift. Increasing the sintering temperature resulted in a clear shift of the XRD peaks of zircon. Microstructural analysis and shifting of XRD peaks showed that Mn element is located all over the zircon grains, assuming to form a solid solution due to its low ion radius and small atomic volume. The solubility limit of Mn in zircon is higher than that of Zn. ZnO also dissolved in zircon; however, because of its higher ion radius and higher atomic volume compared with Mn ions, its solubility was seen at higher temperatures. A secondary phase was observed more in zircon samples containing ZnO than in those containing MnO_2. Both additives inhibited the grain growth of zircon. In this, ZnO was more effective than MnO_2, due to the formation of greater amounts of secondary phase.

ACKNOWLEDGEMENTS

This study was carried out with the financial support of the Iran National Science Foundation (INSF-96008505).

ELECTRONIC SUPPLEMENTARY MATERIAL

The online version of this article (https://doi.org/10.1007/s11837-020-04331-0) contains supplementary material, which is available to authorized users.

REFERENCES

1. M. Awaad and S.H. Kenawy, *Br. Ceram. Trans.* 102, 69 (2003).
2. A. Kaiser, M. Lobert, and R. Telle, *J. Eur. Ceram. Soc.* 28, 2199 (2008).
3. T. Váczi, L. Nasdala, R. Wirth, M. Mehofer, E. Libowitzky, and T. Hager, *Miner. Petrol.* 97, 129 (2009).
4. A.M. Abdelkader, A. Daher, and E. El Kashef, *J. Alloys Compd.* 460, 577 (2008).
5. R. Sarkar and A. Baskey, *Interceram* 60, 308 (2011).
6. M.R. Anseau, J.P. Biloque, and P. Fierens, *J. Mater. Sci.* 11, 578 (1976).
7. M.R. Anseau, J.P. Biloque, and P.J. Fierens, *Mater. Sci. Lett.* 11, 578 (1976).
8. R.S. Pavlik Jr, H.J. Holland, and E.A. Payzant, *J. Am. Ceram. Soc.* 84, 2930 (2001).
9. H. Erkalfa, Z. Misirli, M. Demirci, C. Toy, and T. Baykara, *J. Eur. Ceram. Soc.* 15, 165 (1995).
10. S. Ramesh, W.J. Kelvin-Chew, C.Y. Tan, J. Purbolaksono, A.M. Noor, and M.A. Hassan, et al., *Ceram. Silikáty* 57, 28 (2013).
11. H. Zhou, J. Li, D. Yi, and L. Xiao, *Phys. Proced.* 22, 14 (2011).
12. L. Nikzad, H. Majidian, S. Ghofrani, and T. Ebadzadeh, *Int. J. Appl. Ceram. Technol.* 15, 15 (2017).
13. R.F. Marcomini and D.M.P.F. Souza, *Mater. Res.* 19, 45 (2016).
14. L. Ying, W. Xiuping, Z. Defeng, N. Dezheng, Z. Guanming, and M. Jian, *Adv. Energy Eng.* 2, 61 (2014).
15. P. Babilo and S.M. Haile, *J. Am. Ceram. Soc.* 88, 2362 (2005).
16. Y. Liu and L.E. Lao, *Solid State Ion.* 177, 159 (2006).
17. S.V. Ushakov, W. Gong, M.M. Yagovkina, K.B. Helean, W. Lutze, and R.C. Ewing, *Ceram. Trans.* 93, 357 (1999).
18. T. Geisler, U. Schaltegger, and F. Tomaschek, *Elements* 3, 43 (2007).

19. C. Baudin, F. Cambier, and L. Delaey, *J. Mater. Sci.* 21, 4024 (1986).
20. L. Gao, L. Zhou, C. Li, J. Feng, and Y. Lu, *Optoelectron. Adv. Mater.* 6, 178 (2012).
21. H. Majidian, L. Nikzad, H. Eslami-Shahed, and T. Ebadzadeh, *Int. J. Appl. Ceram. Technol.* 13, 1024 (2016).
22. J. Wang, G. Li, Z. Li, C. Tang, Z. Feng, and H. An, et al., *Sci. Adv.* 3, 1 (2017).
23. B. Johar and Y. Zabar, Proceeding of the MATEC Web of Conferences. *2nd International Conference on Green Design and Manufacture*, 7, 1 (2016).
24. A. Negi, B.S. thesis, Rourkela: National Institute of Technology (2010).
25. M. Valigi, D. Gazzoli, R. Dragone, G. Marucci, and G. Mattei, *J. Mater. Chem.* 6, 403 (1996).
26. J. Hernandez, M.J. Zarate, and G. Rosas, *J. Ceram. Process. Res.* 10, 144 (2009).
27. F. Yang, H. Fang, Q. Hu, C. Zhao, X. Qian, and C. Zhao, *Int. J. Electrochem. Sci.* 12, 8295 (2017).
28. S. Beg, Sarita and P. Varshney, Inorg. Mater., 42, 1083 (2006).
29. M.A. Schubert, S. Senz, and D. Hesse, *Thin Solid Films* 517, 5676 (2009).
30. R.J. Finch and J.M. Hanchar, *Rev. Miner. Geochem.* 53, 1 (2003).
31. B.T. Altıparmak, A. Bouziani, J. Park and A. Oztürk, *19th International Metallurgy & Materials Congress*, vol. 522 (2018).
32. R.F. Marcomini, D.M.P.F. Souza, M. Kleitz, L. Dessemond, and M. Cesar Steil, *ECS J. Solid State Sci. Technol.* 1, N127 (2012).
33. M. Bashir, A. Ashraf, M. Imtiaz, S. Riaz, and S. Naseem, *Advances in nano, biomechanics, robotics and energy research (ANBRE13) world congress*, Korea, vol. 316 (2013).
34. S. Nakayama, S. Kakita, Y. Masuda, and T. Suzuki, *J. Mater. Sci.* 41, 1631 (2006).
35. W. Hume-Rothery, H.M. Powell, and Z. Krist, *Crystall. Mater.* 91, 23 (1935).
36. J.H. Kim and G.M. Choi, *Solid State Ion.* 130, 157 (2000).
37. M. Occhiuzzi, D. Cordischi, and R. Dragone, *Chem. Phys.* 5, 4938 (2003).
38. V.P. Dravid, V. Ravikumar, M.R. Notis, C.E. Lyman, G. Dhalenne, and A. Revcolevschi, *J. Am. Ceram. Soc.* 77, 2758 (1994).
39. S. Ramesh, M. Amiriyan, S. Meenaloshini, R. Tolouei, M. Hamdi, J. Pruboloksono, and W.D. Teng, *Ceram. Int.* 37, 3583 (2011).
40. D.W. Budworth, *Miner. Mag.* 37, 833 (1970).
41. T. Alam, K.H.L. Al Mahmuda, M.F. Hasan, S.A. Shahir, H.H. Masjuki, and M.A. Kalam, et al., *Procedia Eng.* 68, 723 (2013).
42. I.S.A. Farag, I.K. Battisha, and M.M. El-Rafaay, *Indian J. Pure Appl. Phys.* 43, 446 (2005).
43. I.S.A. Farag, M.F. Kotkata, M.M. Selim, I.K. Battisha, and M.M. El-Rafaay, *Egypt. J. Solids* 27, 233 (2004).
44. R.D. Shannon, *Acta. Crystallogr. A* A32, 751 (1976).
45. H. Erkalfa, Z. Misirli, and T. Baykara, *Ceram. Int.* 24, 81 (1998).
46. M. Sathiyakumar and F.D. Gnanam, *Ceram. Int.* 28, 195 (2002).
47. S.M. Kwa, S. Ramesh, L.T. Bang, Y.Y.H. Wong, W.J. Kelvin Chew, C.Y. Tan, J. Purbolaksono, H. Misran, and W.D. Teng, *J. Ceram. Process. Res.* 16, 193 (2015).